Best
Available
Copy

OPTICS RESEARCH: 1975:2

MASSACHUSETTS INSTITUTE OF TECHNOLOGY

PREPARED FOR
DEFENSE ADVANCED RESEARCH PROJECTS AGENCY

31 DECEMBER 1975

ESD-TR-76-34

166069

ADA025338

2

Optics Research

1975

Lincoln Laboratory

MASSACHUSETTS INSTITUTE OF TECHNOLOGY

LEXINGTON, MASSACHUSETTS

Prior Semiannual — A030339

This technical report has been reviewed and is approved for publication.

FOR THE COMMANDER

Eugene C. Raabe, Lt. Col., USAF
Chief, ESD Lincoln Laboratory Project Office

SECURITY CLASSIFICATION OF THIS PAGE (When Data Entered)

REPORT DOCUMENTATION PAGE		READ INSTRUCTIONS BEFORE COMPLETING FORM
1. REPORT NUMBER ESD-TR-76-34	2. GOVT ACCESSION NO.	3. RECIPIENT'S CATALOG NUMBER
4. TITLE (and Subtitle) Optics Research		5. TYPE OF REPORT & PERIOD COVERED Semiannual Technical Summary 1 July – 31 December 1975
		6. PERFORMING ORG. REPORT NUMBER Optics Research (1975:2)
7. AUTHOR(s) Robert H. Rediker		8. CONTRACT OR GRANT NUMBER(s) F19628-76-C-0002
9. PERFORMING ORGANIZATION NAME AND ADDRESS Lincoln Laboratory, M.I.T. P.O. Box 73 Lexington, MA 02173		10. PROGRAM ELEMENT, PROJECT, TASK AREA & WORK UNIT NUMBERS ARPA Order 600 Program Element No. 62301E Project No. 6E20
11. CONTROLLING OFFICE NAME AND ADDRESS Defense Advanced Research Projects Agency 1400 Wilson Boulevard Arlington, VA 22209		12. REPORT DATE 31 December 1975
		13. NUMBER OF PAGES 28
14. MONITORING AGENCY NAME & ADDRESS (if different from Controlling Office) Electronic Systems Division Hanscom AFB Bedford, MA 01731		15. SECURITY CLASS. (of this report) Unclassified
		15a. DECLASSIFICATION DOWNGRADING SCHEDULE

16. DISTRIBUTION STATEMENT (of this Report)

Approved for public release; distribution unlimited.

17. DISTRIBUTION STATEMENT (of the abstract entered in Block 20, if different from Report)

18. SUPPLEMENTARY NOTES

None

19. KEY WORDS (Continue on reverse side if necessary and identify by block number)

optics	optical devices	adaptive mirror
laser technology	optical systems	thermal coupling
thermal blooming		

20. ABSTRACT (Continue on reverse side if necessary and identify by block number)

This report covers work of the Optics Division at Lincoln Laboratory for the period 1 July through 31 December 1975. The topics covered are laser technology and propagation and pollution studies.

Additional information on the optics program may be found in the ARPA/STO Program Semiannual Technical Summary Reports to the Defense Advanced Research Projects Agency.

DD FORM 1473 EDITION OF 1 NOV 65 IS OBSOLETE
1 JAN 73

SECURITY CLASSIFICATION OF THIS PAGE (When Data Entered)

1a

MASSACHUSETTS INSTITUTE OF TECHNOLOGY

LINCOLN LABORATORY

OPTICS RESEARCH

SEMIANNUAL TECHNICAL SUMMARY REPORT
TO THE
DEFENSE ADVANCED RESEARCH PROJECTS AGENCY

1 JULY - 31 DECEMBER 1975

ISSUED 23 APRIL 1976

LEXINGTON   MASSACHUSETTS

ABSTRACT

This report covers work of the Optics Division at Lincoln Laboratory for the period 1 July through 31 December 1975. The topics covered are laser technology and propagation and pollution studies.

Additional information on the optics program may be found in the ARPA/STO Program Semiannual Technical Summary Reports to the Defense Advanced Research Projects Agency.

CONTENTS

INTRODUCTION

I. LASER TECHNOLOGY AND PROPAGATION

A scaling law has been discovered for the limits of phase compensation for multiple-pulse thermal blooming.

Previous results on phase compensation for turbulence have been extended to higher and lower Fresnel numbers.

Multiple-pulse propagation limits with and without phase compensation for atmospheric turbulence have been calculated.

Investigations of fog clearing with high-power pulsed lasers are concerned with the transmission and beam quality of successive laser pulses. In this study a CW probe beam was used to measure the beam quality as a function of time. The probe beam was focused onto a five-element HgCdTe array in order to measure beam quality. The observed effects presently are being examined theoretically.

Two high prf Q-switched lasers were constructed — one passively and the other actively Q-switched. Both were operated at 5-W average power with prf's in excess of 100 kHz.

II. POLLUTION STUDIES

Laser monitoring of atmospheric carbon monoxide (CO) over long ambient paths was performed at two field sites in the St. Louis area for a total of over 40 days, including several weekends. Around-the-clock monitoring was performed much of the time. The raw data have been analyzed and error bars assigned. This work was performed in conjunction with the Environmental Protection Agency for the Regional Air Pollution Study (RAPS).[*]

REPORTS ON OPTICS RESEARCH

1 July through 31 December 1975

PUBLISHED REPORTS

Meeting Speeches

*   *   *   *   *

UNPUBLISHED REPORTS

Journal Article

Meeting Speeches*

---

* Titles of Meeting Speeches are listed for information only. No copies are available for distribution.

ORGANIZATION

OPTICS DIVISION

R. H. Rediker, *Head*
L. B. Anderson, *Associate Head*
M. J. Hudson, *Assistant*
V. H. Rein, *Staff*
S. E. McCarron

ADVANCED TECHNIQUES AND SYSTEMS

S. Edelberg, *Leader*
J. E. Lowder, *Assistant Leader*

Bicknell, W. E.	Henshaw, P. D.	Manlief, S. K.
Blasi, J. T.	Hinkley, E. D.	McSheehy, R. B.
Bradley, L. C.	Keyes, R. J.	Nork, L. P.
Bushee, J. F.	Knowlton, R. C.	O'Neil, R. W.
Dickey, D. H.	Ku, R. T.	Pettingill, L. C.
Ellis, R. H.	Lencioni, D. E.	Thomas, M. A.
Ferdinand, A. P., Jr.	Levine, J. S.	Zwicker, H. R.

OPTO-RADAR SYSTEMS

A. B. Gschwendtner, *Leader*
H. Kleiman, *Assistant Leader*

Becherer, R. J.	Hull, R. J.	McPhie, J. M.
Berger, P. J.	Keicher, W. E.	Merrill, E. R.
Billups, R. R.	Lambert, D. R.	Parenti, R. R.
Cordova, R. J.	Marcus, S.	Tomczak, S. P.
DiMarzio, E. W.	Martin, J. S.	Zieman, H. E.

INFRARED RADAR

R. H. Kingston, *Leader*
P. A. Ingwersen, *Associate Leader*
L. J. Sullivan, *Associate Leader*

Bates, D. H.	Gurski, T. R.	Shey, S. Y.
Bielinski, J. W.	Linder, J. C.	Sullivan, F. M.
Capes, R. N., Jr.	McPherson, R. D.	Swezey, L. W.
Carter, G. M.	O'Donnell, R. G.	Teoste, R.
Daley, J. A., Jr.	Parker, A. C.	Tomasetta, L. R.
Fiasconaro, J. G.	Quist, T. M.	Valcourt, G. L., Jr.
Freed, C.	Sasiela, R. J.	Ziegler, H. L.
Fulton, M. J.	Scouler, W. J.	Zimmerman, M. D.

APPLIED RADIATION

L. C. Marquet, *Leader*
E. S. Cotton, *Assistant Leader*
D. A. Page, *Assistant Leader*
H. A. Pike, *Assistant Leader*

Ariel, E. D.	Johnson, F. B.	Mudgett, D. A.
Bollman, R. A.	Johnson, J. Q.	Perry, F. H.
Braman, C. E.	Johnson, R. E.	Pirroni, J. S.
Brennan, M. J.	Kafalas, P.	Pitts, R. F.
Chaulk, L. W.	Kelsall, D.	Prade, G. C.
Corbosiero, D. M.	Kilcline, C. W.	Primmerman, C. A.
Fouche, D. G.	Kocher, D. G.	Swedberg, J. L.
Grant, P. L.	Kramer, R.	Theriault, J. R.
Greenwood, D. P.	Lifsitz, J. R.	Vernon, H. M., Jr.
Herrmann, J.	Marshall, A. P.	Weaver, L. D.
Huber, E. E., Jr.	Morency, A. J.	

I. LASER TECHNOLOGY AND PROPAGATION

A. PROPAGATION

1. Laboratory Experiment on Phase Correction for Thermal Blooming

New results have been obtained in the laboratory experiment on phase correction for thermal blooming.[1] In this experiment, CW forced-convection-dominated thermal blooming is compensated by using a deformable mirror to add phase corrections to the laser beam. Significant recent accomplishments have included a detailed comparison of experimental and theoretical results and an investigation of the required accuracy of phase-correction schemes.
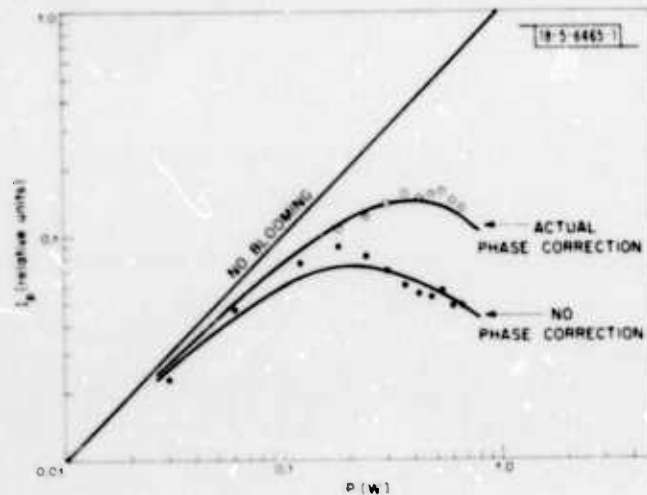
Fig. I-1. Peak focal-plane irradiance vs input power with and without phase correction. The points are experimental results; the solid curves are propagation-code predictions; the straight line would be the irradiance with absorption but no blooming.

Figure I-1 shows a comparison of experimental and theoretical results. (For a complete description of the experimental arrangement, see Ref. 1.) Peak focal-plane irradiance I_p is plotted against input power P, with and without phase correction. The solid points are experimental results with the mirror adjusted to be flat; the circles are experimental results with the deformable mirror adjusted to give maximum improvement. The solid curves are results of the Bradley-Herrmann propagation code calculations for a set of conditions corresponding to those of the laboratory experiment. The lower curve represents no phase correction; the upper curve is a Zernike polynomial representation of the phase profile actually on the mirror. The two sets of results are normalized to the no-blooming curve.

In general, the agreement is good. The main difference occurs in the uncorrected curves, where the experimental data peak slightly higher than the theory predicts. For phase-corrected beams, the agreement is very good, and for the region of significant increase in intensity resulting from phase correction, the propagation code accurately predicts the amount of the increases.

Fig. I-2. Peak focal-plane irradiance vs peak-to-peak mirror deformation.

Fig. I-3. Limit of phase compensation for multiple-pulse thermal blooming (see text); $N_F = 9.4$.

An important question for the practical application of predictive phase-correction schemes is, "How precisely must the phase correction be applied to be effective?" In Fig. I-2, we plot peak focal-plane irradiance at a fixed power against peak-to-peak mirror deformation. The 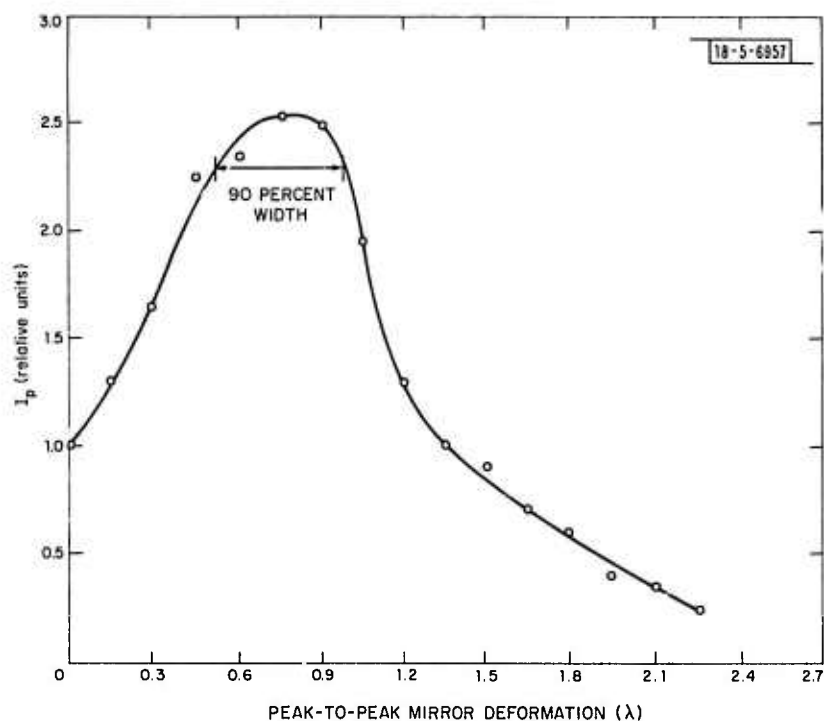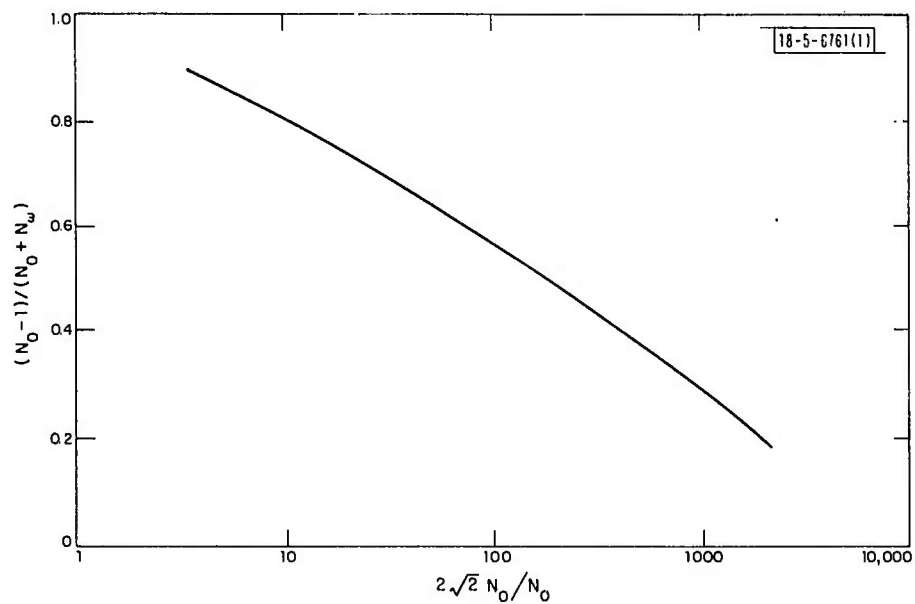irradiance is normalized to one when the mirror is flat, and the relative shape of the phase profile is fixed (see Ref. 1). We observe that for the optimum phase-correction amplitude, the irradiance increases by a factor of 2.5. However, equally important is the width of the curve. We have marked the width at which the irradiance is 90 percent of maximum, and we observe that the mirror-deformation amplitude may vary ±30 percent from optimum, while the irradiance decreases only 10 percent. This result demonstrates that phase corrections do not have to be applied with great precision to be effective.

C. A. Primmerman

2. Phase Compensation for Multiple-Pulse Thermal Blooming

We have found, by a phase-conjugate method, that phase compensation for multiple-pulse thermal blooming is highly effective. Up to a limit that depends on the dimensionless parameters involved, compensation is essentially complete. The limit (which is defined as the point at which optimum compensation leads to a 2-dB loss) can be expressed in a condensed form. The key point is the recognition that the effectiveness of phase compensation depends on how far from the transmitter the perturbation of the medium extends. In an approximation where light rays travel in straight lines, the fraction of the beam length (between transmitter and focus) over which successive pulses overlap is just $(N_0 - 1)/(N_0 + N_\omega)$, where the overlap number $N_0 = D/v\tau$ and the slewing number $N_\omega = \omega R/v$. It is just this fraction of overlap that determines the limit of phase compensation, as can be seen in Figs. I-3 and -4. Here the fraction of overlap $(N_0 - 1)/(N_0 + N_\omega)$ is plotted against the non-dimensionalized energy deposited per pulse, N_D/N_0, for the limit of phase compensation. This limit is defined as the value of N_D (the distortion number) for which the thermal blooming loss, after optimum phase compensation, is 2 dB.
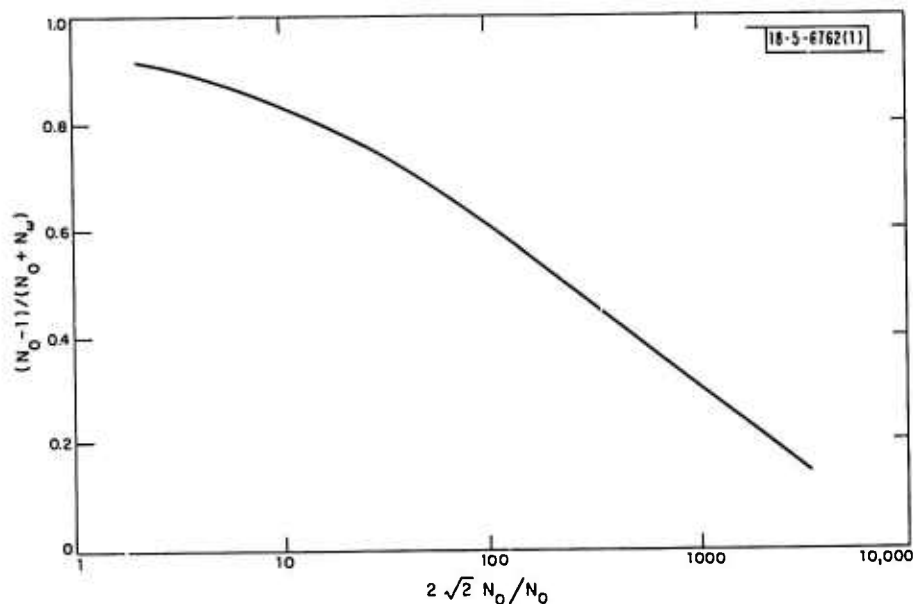
Fig. I-4. Limit of phase compensation for multiple-pulse thermal blooming (see text); $N_F = 18.8$.

3
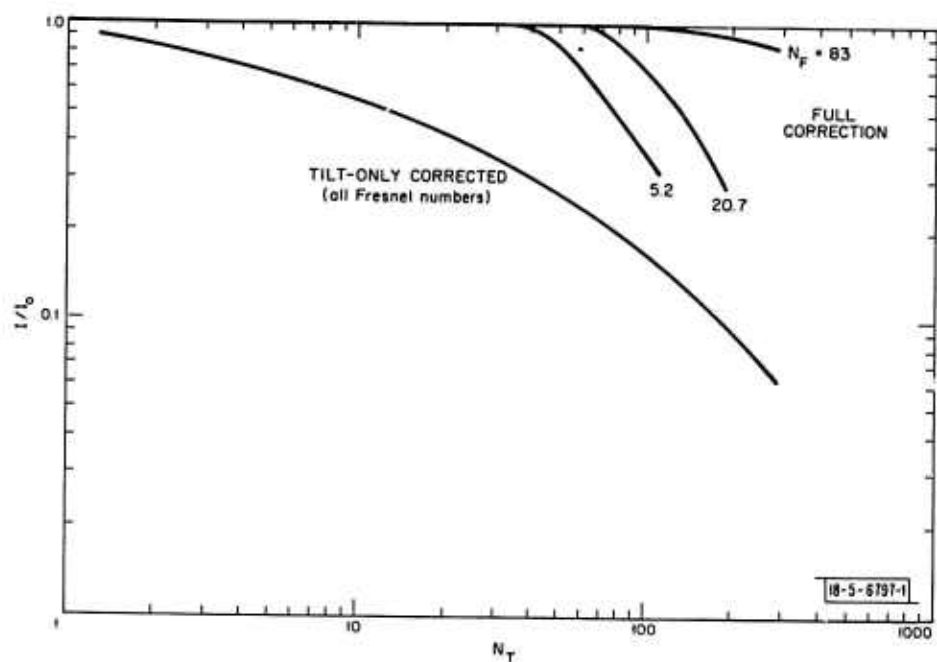
Fig. I-5. Peak irradiance (normalized) as a function of turbulence number N_T $(\equiv k^2 C_n^2 Z a^{5/3})$ for several Fresnel numbers. Lower curve: compensated for tilt-only; upper curves: with full compensation.
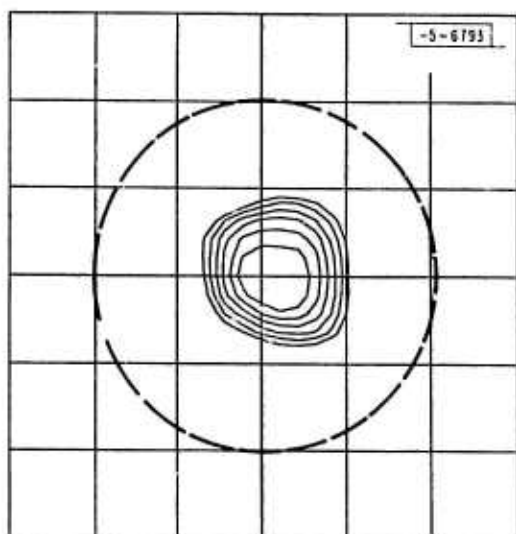
Fig. I-6. Return beam in plane of transmitter for a particular realization. Dashed line shows boundary of transmitter; N_T = 275, N_F = 83.
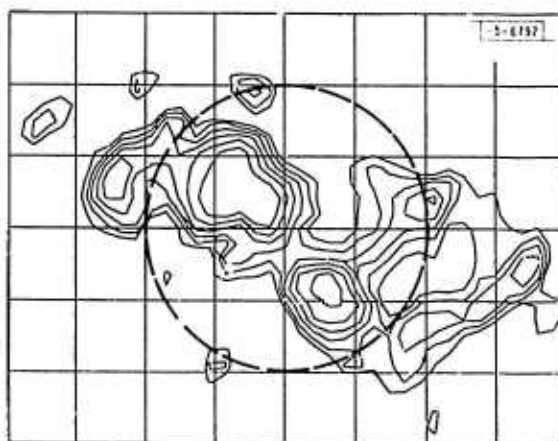
Fig. I-7. Same as Fig. I-6; N_T = 100, N_F = 5.2.

4

The data used in assembling Figs. 1-3 and -4 cover a range of slewing number $0 \leqslant N_\omega \leqslant 8$, and overlap number $1 < N_o \leqslant 100$, but in these plots the whole range of these variables falls on a single line (for each Fresnel number). The two Fresnel numbers are plotted on the two separate figures; if plotted on a single graph the lines for the two Fresnel numbers would almost, but not quite, coincide. The difference (a slightly lower curve at high fractional overlap for the low Fresnel number) corresponds to the larger departure from geometrical paths for the lower Fresnel number.

The above curves correspond to Gaussian beams truncated at the $1/e^2$ power radius. We have tried a few cases with different beam shapes. For uniformly illuminated circular or square apertures, the limits of compensation were very nearly the same as for the truncated Gaussian. (In computing the dimensionless numbers for the square, the side of the square, rather than the diagonal, was used as the beam diameter, and the wind and slewing were taken parallel to the side.)

<div style="text-align:right">

L. C. Bradley
M. G. Cheifetz

</div>

3. Phase Compensation for Turbulence

In a meeting speech at the Optical Society of America,[1] we presented the results of calculations on phase compensation for turbulence, showing that beyond a certain level of turbulence such correction was ineffective. These calculations were performed for a single Fresnel number. We have now extended these calculations to higher and lower Fresnel numbers in an attempt to ascertain the dependence on this quantity. Figure I-5 shows the results. It will be seen that although all Fresnel numbers give the same beam degradation with tilt-only corrected, the beams with high Fresnel number can be corrected more readily than those with low Fresnel number.

The difference is attributable to the difference in behavior of the return beam. Figure 1-6 shows isoirradiance contours for the return beam for the high Fresnel number; it will be seen that there is very little distortion of this beam, and reference to Fig. I-5 shows that the correction here is nearly complete. In contrast, Fig. I-7 shows the contours for the low Fresnel number; the return beam is highly distorted (scintillation is approaching saturation), and the correction is much less successful.

<div style="text-align:right">

L. C. Bradley
M. G. Cheifetz

</div>

4. Fog Hole Boring and Propagation Study

a. Introduction

Investigations of fog clearing with high-power pulsed lasers are concerned with the transmission and beam quality of successive laser pulses. Both theoretical[2] and experimental studies of transmission[3] have been conducted. Beam quality, on the other hand, has not been studied as extensively. Previous experimental work[4] in fog clearing has made use of a focused clearing beam in order to achieve the required energy density necessary for clearing. The beam quality was studied by using a second high-power pulse as a probe beam. When this method is used, the spreading of the probe beam is measured at one point of time for each shot. Since there are several possible effects which may contribute to the measured beam quality, the true cause of effects observed at a single point in time may be difficult to determine. We hope to separate these effects in two ways. First, by measuring the beam quality and transmission as

a function of time using a CW probe laser, we hope to separate effects which operate on different time scales. Second, by changing the clearing beam geometry from focused to collimated, we hope to minimize one possible effect, the diffraction of the probe beam due to the small diameter of the cleared path.

b. Experimental Setup

The experimental setup is shown in Fig. I-8. The 10.6-μm pulsed laser supplied the clearing beam. This beam was directed by a turning flat to the Ge beam splitter, where it was combined with the probe beam. The reflection from the beam splitter was directed through a
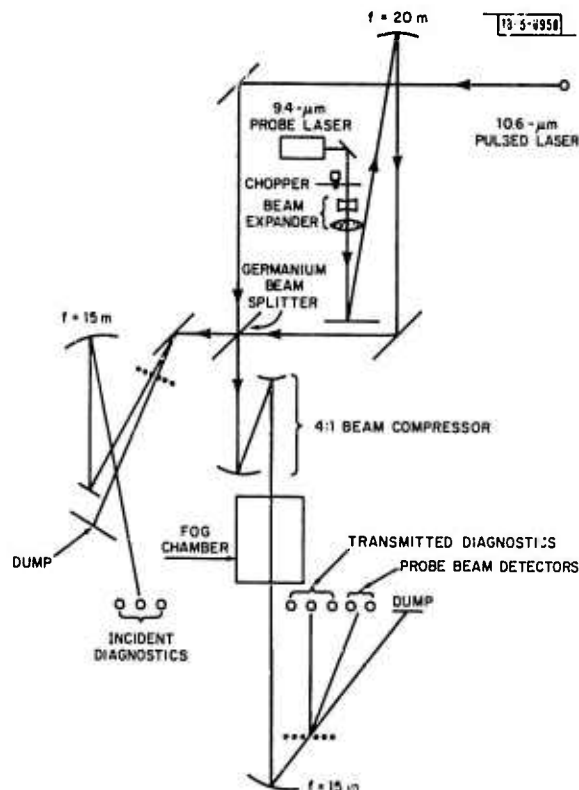

Fig. I-8.　Experimental setup for examination of fog clearing.

grating, and the third, fourth, and fifth orders were used as input diagnostics, consisting of two barium titanate detectors and one photon drag detector. A tunable CO_2 laser, operating at 9.4 μm, was used as the probe beam. This beam was chopped at 300 Hz, expanded to 8-cm diameter using two Ge lenses, and collimated with a 20-m mirror. This beam was directed to the Ge beam splitter with a turning flat where the reflection from the beam splitter was combined with the 10.6-μm clearing beam. The transmitted 9.4-μm beam was dumped. At the output of the beam splitter, the 8- $\times$ 14-cm, 10.6-μm beam and the 8-cm-diameter probe beam were collimated and traveling downrange along the same path. These beams were compressed using a two-mirror confocal-beam compressor which raised the energy density of the 10.6-μm probe beam by a factor of 16. They were then propagated through a 5-m fog cell. The transmitted beams were focused using a 15-m mirror, and the output diagnostics were placed in the focal plane. Two barium titanate calorimeters and a photon drag detector were placed in the

third, fourth, and fifth orders to measure the 10.6-μm beam, and two sets of detectors were placed in the first and second orders of the 9.4-μm beam in order to measure the probe beam. The probe beam diagnostics were composed of a large area Au:Ge detector to measure the total probe beam transmission, and a five-element HgCdTe array to measure the beam spreading. The array elements measured 0.7 × 1 mm, and their center-to-center distance was 2 mm. The output of all six detectors was recorded with a Visicorder.

c. Experimental Procedure

At the beginning of each run, the five-element array was centered on the probe beam. The Visicorder was started with no fog in the chamber to determine a baseline. As the fog was brought up, the transmission of the 9.4-μm beam was monitored on an oscilloscope. When the fog reached the desired level, the Visicorder was run at 0.1 sec/inch and the clearing pulse was fired. The fog was then turned off, and the Visicorder was run at 10 sec/inch until the transmission returned to the pre-fog level. Thus, a complete record of several minutes surrounding each shot was obtained. The clearing pulse energy and pulse shape were recorded for each shot for both incident and transmitted beams.

d. Preliminary Results

A typical set of Visicorder traces during the time surrounding the shot is shown in Fig. I-9. The detectors were numbered as shown. Detector 2 of the HgCdTe array was turned off due to noise considerations. The array traces show an increase in transmission and an increase in the

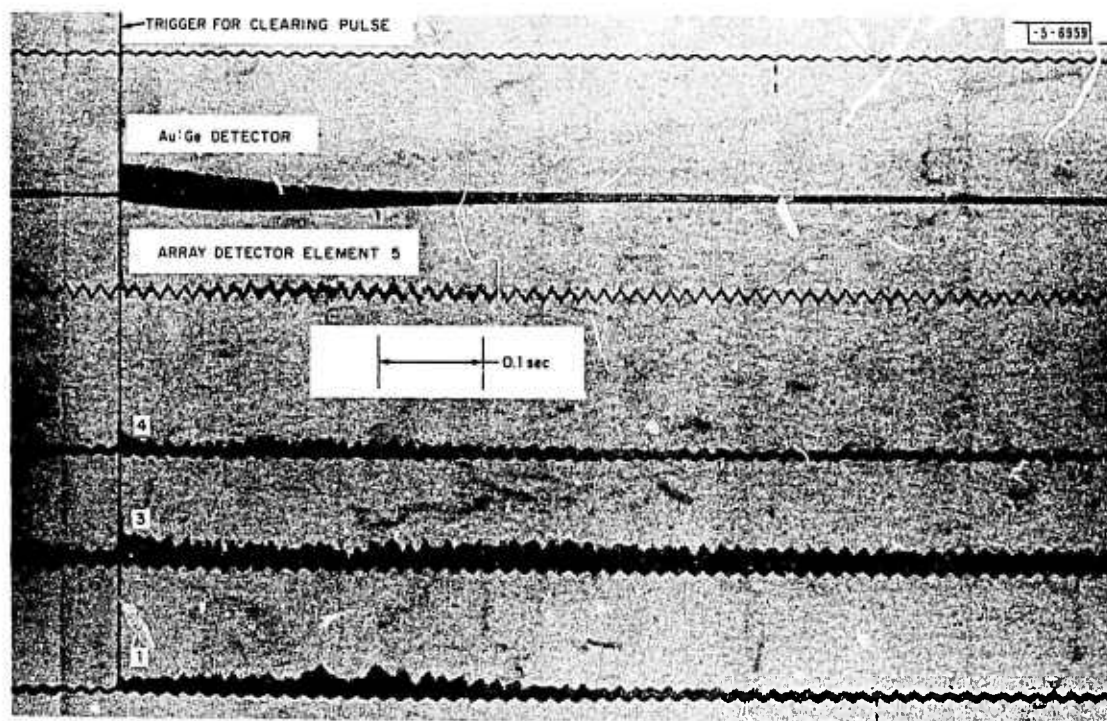Fig. I-9. Typical Visicorder trace showing transmission of the probe beam through the fog cell as a function of time and position. (Array elements 1, 3, 4, and 5 are shown. The Au:Ge detector monitored total transmission integrated over position.)
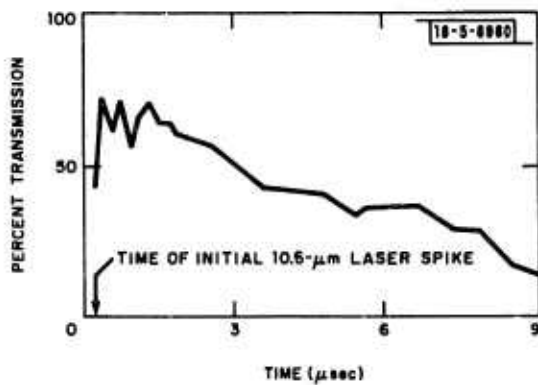
Fig. I-10. Transmission of the clearing pulse vs time as measured by incident and transmitted photon drag detectors.
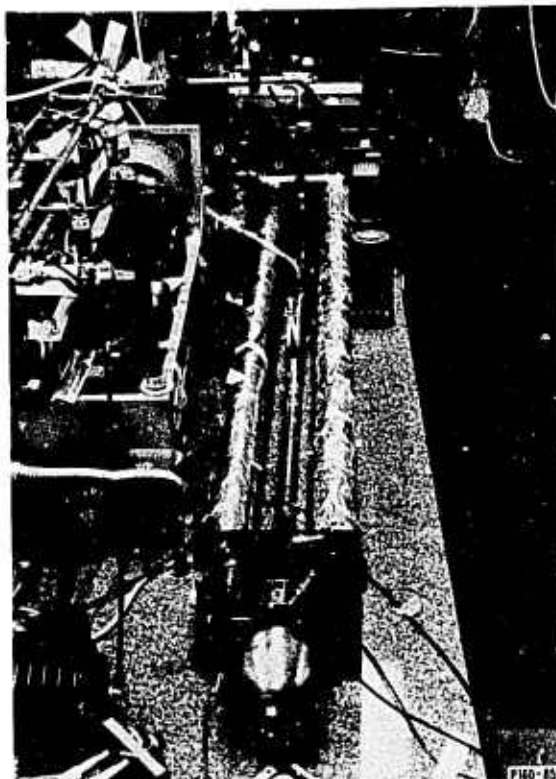

Fig. I-11. Passively Q-switched CO_2 laser.

focal spot size. Other shots show larger signals on the outside detectors than on the center of the array. These effects might be due to beam spreading caused by either turbulence or blooming. Another cause of this effect might be uneven clearing of the fog, due to hot spots in the 10.6-μm clearing pulse. This possibility presently is being examined theoretically.

The amount of clearing, as measured by the Au:Ge detector, was always less than 100 percent, even when the incident energy was much greater than the clearing energy. This agrees with results published earlier.[3]

An interesting result has been observed from examination of the incident and transmitted photon drag traces. These produce a time-resolved trace of the laser power during the pulse. By taking the ratio of the incident and transmitted diagnostics, the transmission of the clearing pulse can be plotted vs time. A typical result is shown in Fig. I-10. In all cases, the spike transmission is low, the main pulse transmission goes up as if clearing had taken place, and then the transmission drops off. An examination of background shots showed that this effect is only present when there is fog in the chamber. A possible explanation for this phenomenon is the presence of moving hot spots in the laser beam. When the laser power shifts its spatial distribution during the pulse, the effect would be as if the laser were propagating through an uncleared medium. Since the second part of the pulse has much lower power, it would not be powerful enough to clear a hole for itself.

A visual effect was observed which has not been investigated experimentally. When visible light scattered by the fog is observed during the shot, greater scattering is observed from the bored hole. This indicates the possible creation of small droplets in the beam, and should be examined further, both experimentally and theoretically.

<div align="right">

P. D. Henshaw   S. K. Manlief

D E. Lencioni   R. B. McSheehy

</div>

B. HIGH PRF Q-SWITCHED CO_2 LASERS

During this reporting period, work was initiated on the development of high pulse-repetition-frequency (prf) Q-switched CO_2 lasers. The design goal was 5 to 10 W of TEM_{oo} average power at a prf of 10^5 Hz, with a pulse width of less than 0.5 μsec. Two Q-switching approaches were taken — one passive and one active — both of which met these requirements.

The passively Q-switched laser, shown in Fig. I-11, is a modification of the stable, sealed-off CW lasers previously reported.[5] Laser line selection is accomplished by means of a diffraction grating as one of the cavity end reflectors. In addition, the Q-switching version incorporates an intracavity stainless steel cell shown in Fig. I-12, which contains a saturable absorbing gas. The saturable absorber which we have used to date is sulfur hexafluoride (SF_6) diluted with helium. This mixture has been demonstrated to be an efficient Q-switcher of the high-gain lines in the P-branch of the 10.6-μm band.[6] The purpose of the helium diluent is to regulate the recovery time of the SF_6 absorber and, consequently, the prf of the laser. Typical partial pressures are 0.01 Torr SF_6 and 5 Torr He.

Figure I-13 shows a passively Q-switched pulse train with a prf of slightly greater than 100 kHz as well as an individual pulse. For this mode of operation the average power output was 5.5 W.

By adjusting the helium pressure, the prf could be varied over a considerable range, with frequencies in excess of 150 kHz observed. This prf is to our knowledge the highest reported for
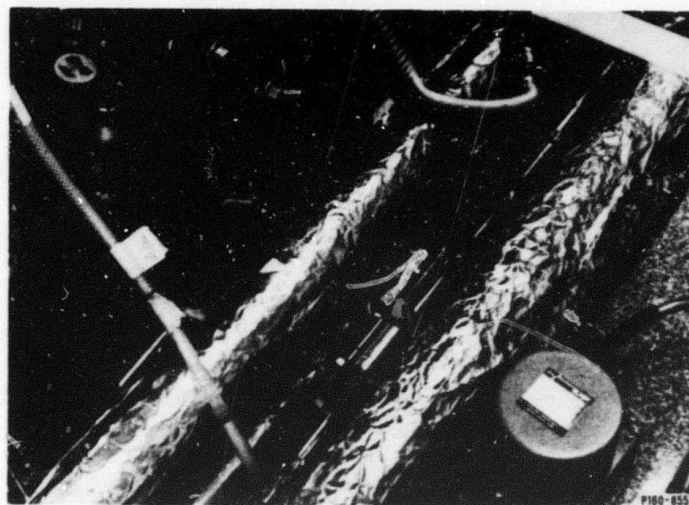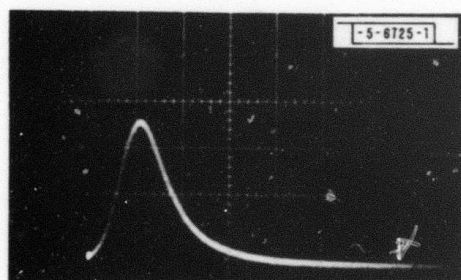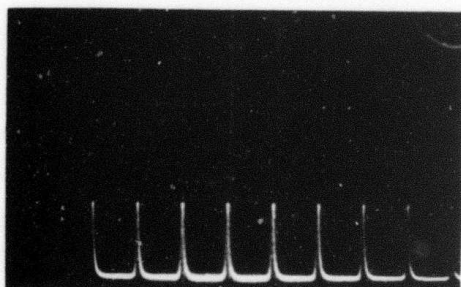
Fig. I-12. Intracavity absorption cell.

(a)

→| |← 0.5 μsec

(b)

→| |← 10 μsec

Fig. I-13. Passively Q-switched laser pulses at prf of ~100 kHz: (a) individual pulses and (b) pulse train.
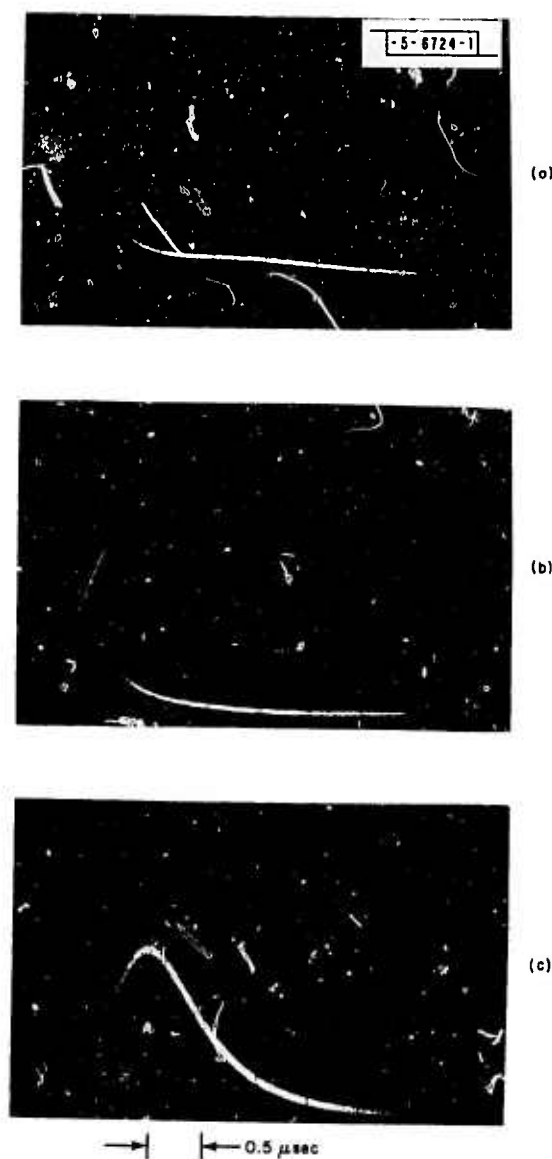
10

Fig. I-14. Passively Q-switched laser pulse shapes for various prf's:
(a) prf = 12 kHz, (b) prf = 40 kHz, and (c) prf = 140 kHz.

a passively Q-switched CO_2 laser. As shown in Fig. I-14, however, operating at very high prf's results in a substantial increase in pulse width. This is due to the fact that the laser gain does not recover completely between pulses and therefore requires a longer time to saturate the SF_6, thus broadening the pulse.

As yet, only P(20) of the 10.6-μm band has been studied. Many other lines of both normal and isotopic CO_2 can be Q-switched using SF_6, as well as other absorbing gases.[7-9]

As an alternative approach, a second Q-switched laser was built, which employs a multi-apertured rotating wheel as an intracavity Q-spoiling mechanism. The aluminum wheel is 4.5 inches in diameter and contains 300 equally spaced milled slots each 0.008 inch wide. It is located at the common focus of a 1.5-inch focal length ZnSe lens pair and driven by a
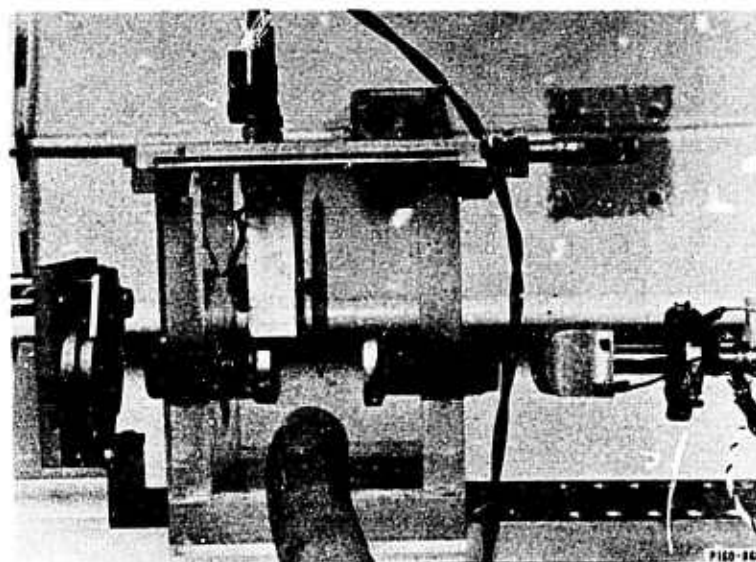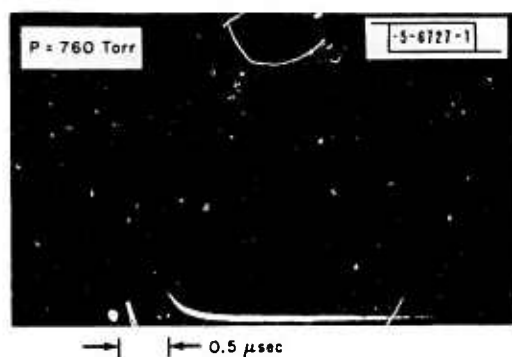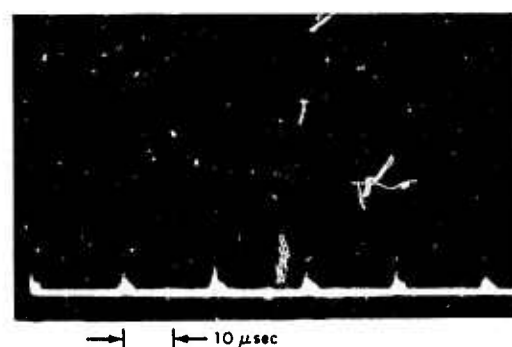
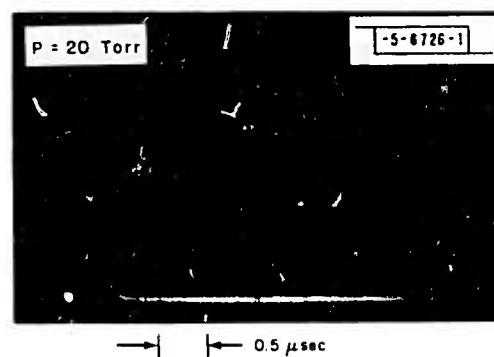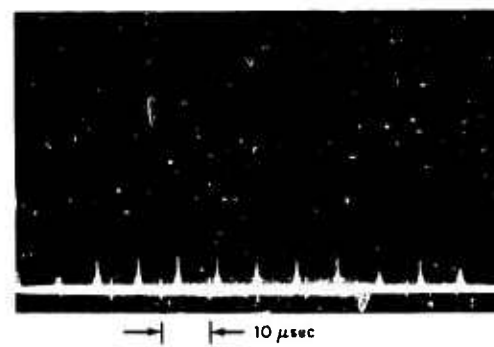Fig. I-15.   Rotating wheel Q-switch.

Fig. I-16.   Actively Q-switched laser pulses with rotating wheel at atmospheric pressure: (a) individual pulse and (b) pulse train.

Fig. I-17.   Actively Q-switched laser pulses with rotating wheel at 20-Torr pressure: (a) individual pulse and (b) pulse train.

20,000-rpm DC motor. In order to eliminate air drag on the wheel, the wheel-motor assembly was housed in a Plexiglas vacuum enclosure whose windows are the ZnSe lenses. As shown in Fig. 1-15, the position of both lenses and the wheel can be continuously adjusted to optimize output.

Figure 1-16 shows an individual pulse and pulse train at the highest attainable prf at 760 Torr. The average TEM_{00} power output was measured at 5 W. At atmospheric pressure, the motor could drive the wheel at only half its rated speed, resulting in a prf of approximately 50 kHz. Even at this speed, however, the switching is considerably faster than in the passively Q-switched laser. This is evidenced by the significantly narrower pulses provided by the rotating wheel.

When the enclosure was evacuated to 20 Torr, the motor could then drive the wheel at its rated speed. As shown in Fig. 1-17, this resulted in a prf of 120 kHz, which to our knowledge is the highest prf reported for a mechanically Q-switched laser. Reducing the ambient pressure below 20 Torr resulted in no significant further prf increase. The average power at 120 kHz was also 5 W, implying that by doubling the prf we halved the peak pulse power.

The irregular pulse heights in Fig. 1-17 are due in combination to the facts that (1) at this high prf, the laser gain does not fully recover between pulses and (2) the widths of the milled slots are not precisely uniform. This condition should be ameliorated by using a more accurate photo-etched wheel. Such a wheel has been fabricated and will be tested shortly.

C. Freed
S. Marcus

REFERENCES

1. L. C. Bradley et al., "Limits of Phase for Turbulence," Optical Society of America, Boston, 21-24 October 1975.

2. S. L. Glickler, Appl. Opt. 10, 644 (1971).

3. J. E. Lowder, H. Kleiman, and R. W. O'Neil, J. Appl. Phys. 45, 221 (1974).

4. Optics Research Report, Lincoln Laboratory, M.I.T. (1975:1), DDC AD-A020339.

5. C. Freed, IEEE J. Quantum Electron. QE-4, 404 (1968).

6. O. R. Wood and S. E. Schwarz, Appl. Phys. Lett. 11, 88 (1967).

7. S. Marcus, Appl. Phys. Lett. 15, 217 (1969).

8. J. T. Yardley, Appl. Phys. Lett. 12, 120 (1968).

9. N. V. Karlov, G. P. Kuzmin, Yu. N. Petrov, and A. M. Prokhorov, JETP Lett. 7, 134 (1968).

II. POLLUTION STUDIES[*]

A. ATMOSPHERIC CO MONITORING OVER LONG PATHS IN THE 1975 REGIONAL AIR POLLUTION STUDY (RAPS) IN ST. LOUIS

1. Introduction

During the period from 7 July to 10 September 1975, our tunable diode laser system for long-path monitoring of atmospheric carbon monoxide (CO) was stationed in St. Louis, in conjunction with the RAPS program sponsored by the U.S. Environmental Protection Agency. The system, housed in a mobile van, was located at Site 108 (Granite City, Illinois) for the first half of the program, to 4 August, and then moved to Site 105 (inner St. Louis) for the duration.

Approximately 40 days of long-path monitoring were obtained, including several around-the-clock periods and weekends. A great deal of time was spent in validating the calibration to establish quality assurance of the data. This was done to insure the accuracy of the laser data for future entry to the data bank at EPA.

The long-path results were compared with RAMS (Regional Air Monitor Station) readings from a Beckman 6800 gas chromatographic instrument, and with an advanced commercial prototype gas-filter-correlation (GFC) instrument located inside the van. The GFC instrument, developed by Aeronutronic Ford, was capable of continuous point monitoring of ambient CO.

The commercial $PbS_{1-x}Se_x$ diode laser was chemically tailored to emit laser radiation from 2103 to 2107 cm^{-1} (4.75-µm region) in the fundamental absorption band of CO. The monitoring technique was that of resonance absorption. The diode laser system and measurement techniques have been described in detail in previous Optics Research Reports.[†‡] RAPS-75 measurement results will be presented below.

2. Site 108 – Granite City, Illinois

During the period from 7 July to 4 August, the laser monitoring van was located next to the RAMS on this rural site, shown in Fig. II-1. Because of its remote location, there is little vehicular traffic to influence the CO concentration at this site. However, with the winds from the southwest quadrant, pollution from the St. Louis metropolitan area can become a factor; and from the southerly direction, pollution from vehicular traffic and industries in Granite City is present.

Figure II-2 shows a typical 24-hour monitoring period at Site 108. The continuous trace represents the long-path laser result replotted with a 30-sec time constant from the original data. The hourly averages of the RAMS and GFC readings are also shown, as crosses and circles, respectively, for comparison. Fairly good agreement is obtained between these measurements on this day of very low CO concentration. Calibrations of the laser system are indicated by the letter "C" at the appropriate times. A 10-percent calibration fluctuation occurred during the 24-hour period. Figure II-3 illustrates interesting CO results obtained on
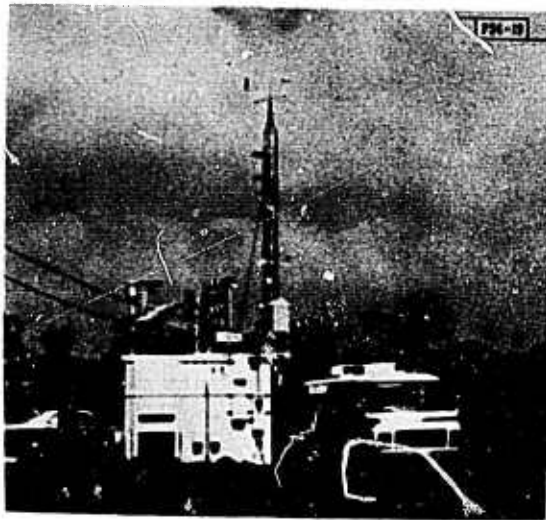
Fig. II-1. Photograph of Site 108 at Granite City, Illinois, with laser monitor van stationed next to RAMS.
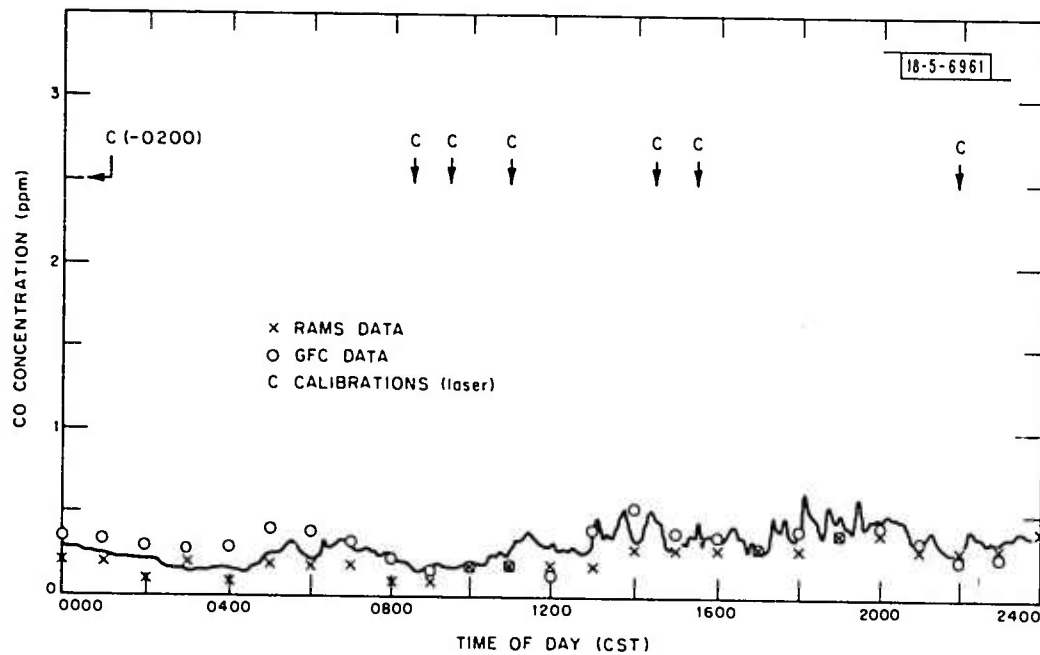

Fig. II-2. Around-the-clock CO monitoring on 1 August 1975 at RAMS Site 108. Distance to retroreflector = 0.34 km; monitoring direction, north; calibration accuracy = ±10 percent; zero drift = 0.05 ppm.
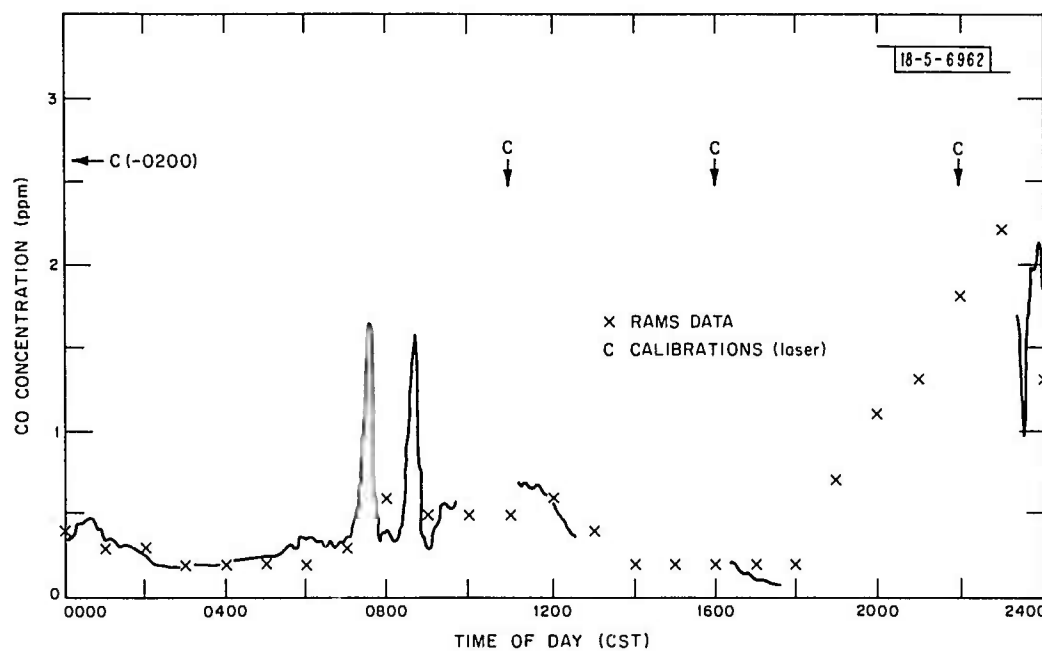
Fig. 11-3. Long-path CO monitoring at RAMS Site 108 on 2 August 1975. Distance to retroreflector = 0.34 km; monitoring direction, north; calibration accuracy = ±5 percent; zero drift = 0.00 ppm.

2 August 1975. Two sharp peaks were recorded by the laser monitor around 0800 CST. Due to the rapid, large fluctuations of the CO concentration, agreement with the RAMS hourly averages at 0800 and 0900 CST is poor. Excellent correlation is shown, however, for this period in Fig. 11-4 when the minute-by-minute averages of the RAMS data are compared with the original laser data having 1-sec time constant.

A total of 21 days of long-path CO measurements was obtained at this site. Data correlation with meteorological results is in progress.
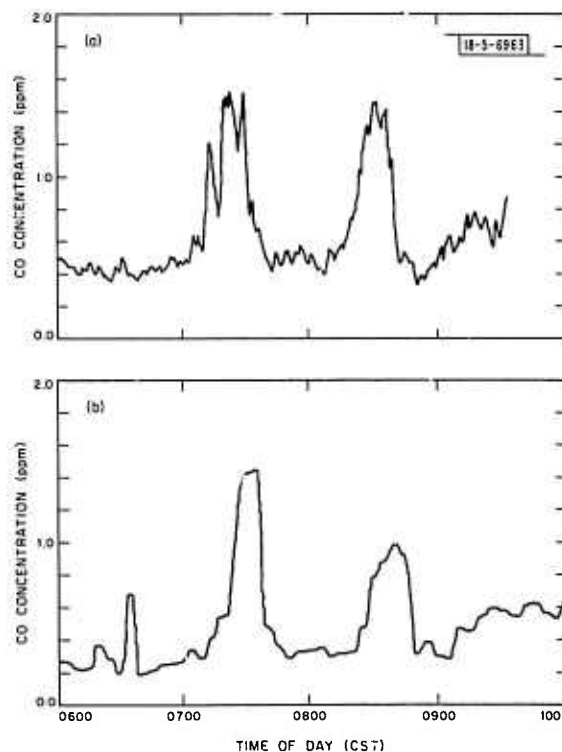

Fig. II-4. Comparison of CO monitoring results, from 0600 to 1000 CST on 2 August at RAMS Site 108, between (a) the long-path laser monitor and (b) RAMS Beckman 6800 gas chromatograph. Time constant is 1 sec for (a) and 1 minute for (b).

17

3. Site 105 – Downtown St. Louis, Missouri

Carbon monoxide concentrations were monitored at this site from 6 August to 10 September 1975. Figure II-5 shows typical results of these measurements over a 0.65-km path (1.3-km round trip), to the top of the Monsanto Building shown in Fig. II-6, between 0000 and 0800 hours CST. In the afternoon, the path length was reduced to 0.13 km and directed in the opposite direction (southerly). The hourly averages of RAMS CO readings are shown again as crosses in Fig. II-5 for comparison purposes. Two significant discoveries were made at this site: (a) There were several unknown absorption lines close to the laser frequency used for monitoring CO and (b) there was a slow, steady drift in laser frequency over a period of time, apparently caused by changes in line voltage during periods of heavy air conditioner usage.

The absorption line of the interfering species was located between the CO P(9) line at 2107 cm^{-1} and the CO P(10) line at 2103 cm^{-1}. The unknown species probably came from the industries around Site 105, since it was not in evidence at Site 108, the farm site in Illinois. In addition, recent laboratory tests showed that automobile exhausts contained no such interference. During the monitoring period, whenever this interference occurred, we reduced the path length to 100 to 200 m in order to permit laser operation at line center, and thus minimize this effect. A new diode laser chemically tailored to the interference-free region of 2127 to 2133 cm^{-1} will have to be used in the future to completely eliminate this interference problem.

With regard to the observed drift in laser frequency at Site 105, we found that the calibration changed by a factor of 2 between 0800 to 1700 CST. Such a large drift in calibration usually occurred during the daytime; the drift was usually lowered to 10 to 20 percent during evening monitoring periods, which is comparable with that observed at Site 108.
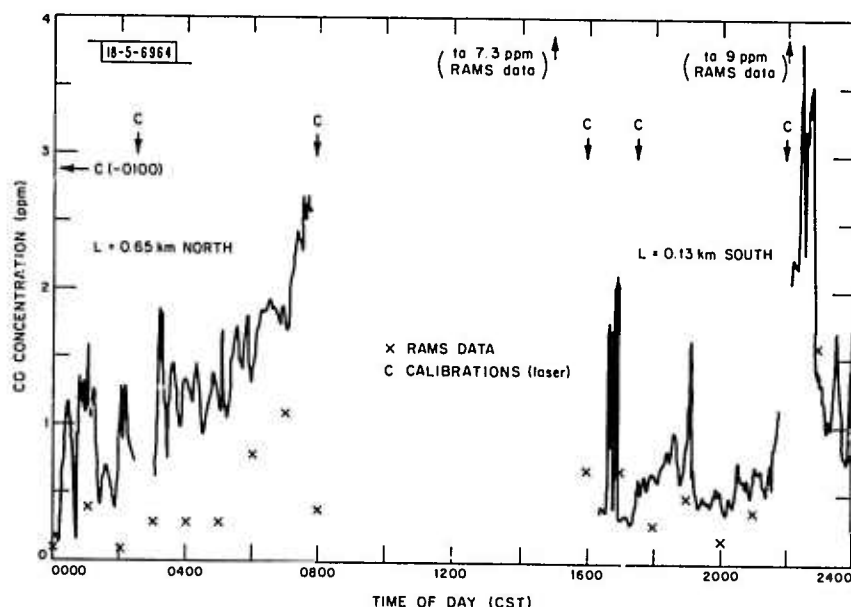

Fig. II-5. Long-path CO monitoring at RAMS Site 105 on 27 August 1975. Distances to retroreflector = 0.65 and 0.13 km in northerly and southerly directions, respectively; calibration accuracy = ±5 percent (0000 to 0800 CST), ±20 percent (1600 to 2400 CST); zero drift = ±0.07 ppm (0000 to 0800 CST), ±0.04 ppm (1600 to 2400 CST).

Fig. II-6. Photograph taken at RAMS Site 105 in downtown St. Louis from van toward top of Monsanto Building. Distance = 0.62 km (one of the laser monitoring paths).
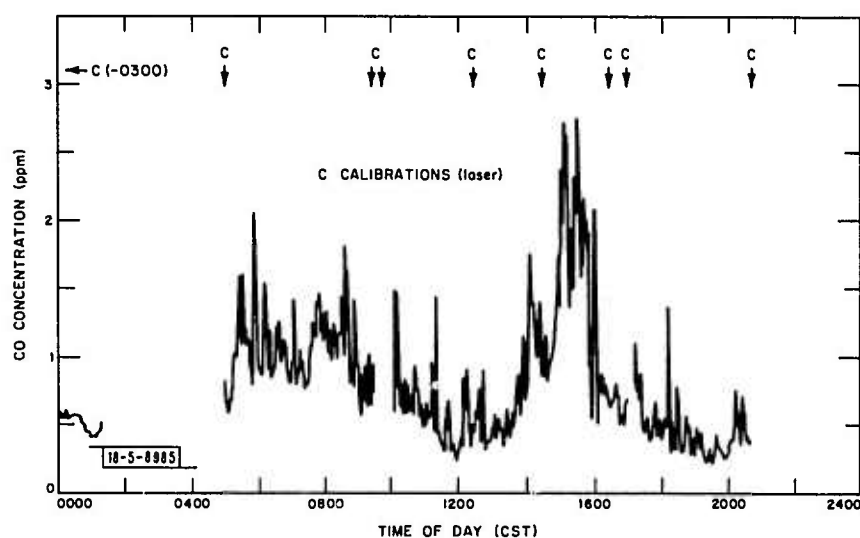

Fig. II-7. Long-path CO monitoring at RAMS Site 105 on 10 September 1975 with AFC circuit installed. Distance to retroreflector = 0.13 km; monitoring direction, south; calibration accuracy = ±5 percent; zero drift = 0.04 ppm.

Calibration drift was reduced considerably at Site 108 by locking the laser frequency onto the same CO absorption line used for the ambient-air monitoring with the aid of a secondary calibration cell and infrared detector. A feedback circuit was used to supply an additional control current (of up to 5 mA) to the laser in order to stabilize its frequency. Calibration drift on the order of ±2 percent was observed over 25 hours with this control scheme. Figure II-7 shows results of monitoring on 10 September 1975, after the automatic frequency control (AFC) circuit was installed. Data uncertainty was reduced to ±5 percent as a result of this AFC circuit.

R. T. Ku
E. D. Hinkley